# Performance Assessment of Variational Integrators for Thermomechanical Problems

Dominik Kern*
*Chair of Applied Mechanics and Dynamics,*
*TU Chemnitz, Germany*

Ignacio Romero
*ETSI Industriales, Technical University of Madrid, Spain*
*IMDEA Materials, Getafe, Spain*

Sergio Conde Martín and Juan Carlos García-Orden
*ETSI de Caminos, Canales y Puertos, Technical University of Madrid, Spain*
(Dated: October 28, 2016)

Structure-preserving integrators are in the focus of ongoing research because of their distinguished features of robustness and long time stability. In particular, their formulation for coupled problems that include dissipative mechanisms is still an active topic. Conservative formulations, such as the thermo-elastic case without heat conduction, fit well into a variational framework and have been solved with variational integrators, whereas the inclusion of viscosity and heat conduction are still under investigation. To encompass viscous forces and the classical heat transfer (Fourier's law), an extension of Hamilton's principle is required. In this contribution we derive variational integrators for thermo-viscoelastic systems with classical heat transfer. Their results are compared for two discrete model problems vs. Energy-Entropy-Momentum methods. Such comparisons allow to draw conclusions about their relative performance, weaknesses and strengths.

arXiv:1610.08666v1 [physics.comp-ph] 27 Oct 2016

## I. INTRODUCTION

In mechanics, Variational Integrators (VI) and Energy-Entropy-Momentum (EEM) methods are the current state of the art in structure preserving time integration. Both of these families of methods have been used for over two decades in many applications and have consistently demonstrated their ability to solve evolution equations in a robust and accurate manner. Although completely different in their genesis and background, they pursue the same goal of accurate structure preservation, and compete as they are applied to ever more general theories.

The concept of VI was introduced by Cadzow [3] in the seventies and comprehensively developed by the group at Caltech and worked out many special cases (see the overview [14]). The basic idea is to start the discretization directly from the variational principle, thus skip the formulation of differential equations and lead to one-step maps, which are implicitly determined by algebraic equations. Originally developed for conservative systems, their extension to dissipative effects is currently being researched (c.f. the recent works [12, 17]). Viscosity and heat transfer are such effects of technical relevance in order to account for damping and temperature effects. The geometric consequence of dissipation is the loss of symplecticity, however the performance of VIs does not deteriorate. They are robust and by design at least second-order accurate. Typical applications are in astronomy and space mission design, and increasingly in robotics, where VIs offer practical advantages for feedback control.

* dominik.kern@mb.tu-chemnitz.de

EEM methods were introduced by Romero [21] and utilize the discrete derivative operator [7], initially developed for the Energy-Momentum method (EM) [24], to build thermodynamically consistent algorithms from the *geometric* structure revealed by the GENERIC formalism [20]. Such formalism enables a unified expression of the evolution equations of any isolated thermodynamic system to be generated from the addition of the reversible and irreversible parts, which are directly related to the gradient of the total energy and the total entropy of the system in terms of the state vector, respectively. Due to the key properties of the discrete derivative operator, the resulting methods are automatically second-order accurate, energy-preserving and entropy-producing by design. In addition, first order accurate staggered methods could also be formulated in terms of entropy in such a way that each step remains thermodynamically consistent, see also [21]. Within this approach, different thermomechanical systems have successfully been addressed in terms of the so called entropy-based formulation, i.e using entropy as thermodynamic state variable, such as discrete thermoelasticity [21], discrete thermo-viscoelasticity [6] and continuos nonlinear thermoelasticity [22, 23] with heat transfer. Very recently, a temperature-based formulation for discrete thermo-elasticity has been proposed in [16], overcoming the problems associated to the use of the entropy and hence fully complementing the GENERIC-based approach.

The purpose of this contribution is the assessment of the precision and robustness of variational integrators, in comparison to EEM methods and focusing on their conservation properties. To this end, the paper is structured as follows. In section II the problem of thermomechanical systems is defined in general. In section III the time

discretization is described, namely a VI and two EEM schemes, namely the energy-entropy-momentum method in entropy and in temperature formulation. In section IV these integrators are compared with each other at two discrete systems, a planar single and a spatial double pendulum. Section V concludes this performance assessments.

## II. PROBLEM DEFINITION

In this article we consider thermo-viscoelastic models possessing a Lagrangian

$$L = T(\mathbf{q}, \dot{\mathbf{q}}) - \psi(\lambda, \gamma, \vartheta), \tag{1}$$

where $T$ denotes kinetic coenergy (the distinction between kinetic energy and coenergy is in the spirit of Crandall [4]) and $\psi$, the free energy function (Helmholtz free energy). The structure of the free energy

$$\psi(\lambda, \gamma, \vartheta) = (1 + \beta_c)\psi_e + \mu\gamma^2 - \beta_c\gamma\frac{\partial\psi_e}{\partial\lambda} \tag{2}$$

is adopted from Holzapfel and Simo [10]. This kind of models are referred to as generalized Maxwell-elements and may be represented as rheological model of a thermo-elastic spring (main spring), characterized by the free energy $\psi_e(\lambda, \vartheta)$, in parallel with a combination of another thermo-elastic spring in series with a dash-pot (see fig. 1). Sometimes it is also referred to as Poynting-element by some authors [2]. It may be used either as infinitesimal line element for the construction of a continuum model or as component of a discrete model. This element is described by three state variables, namely, the total stretch $\lambda$, the viscous stretch $\gamma$ and its temperature $\vartheta$. For the temperature it will turn out useful to formulate it as time derivative $\vartheta = \dot{\alpha}$ of a quantity called thermacy $\alpha$, which is also referred to as "thermal displacement", since temperature $\vartheta = \dot{\alpha}$ is related with the averaged velocity of atoms (strictly speaking their averaged kinetic energy). The corresponding momenta are the mechanical momentum $\mathbf{p}$ and the entropy $s$

$$\mathbf{p} = \frac{\partial L}{\partial \dot{\mathbf{q}}}, \tag{3a}$$

$$s = \frac{\partial L}{\partial \dot{\alpha}} = -\frac{\partial \psi}{\partial \dot{\alpha}}. \tag{3b}$$

Due to the similarities of these two definitions, the entropy is sometimes referred to as "thermal momentum". The viscous stretch is related with a vanishing momentum variable, as its time derivative $\dot{\gamma}$ does not enter the Lagrangian. The quantities conjugated to the deformation variables are total internal force $f$ and its viscous component $g$

$$f = \frac{\partial \psi}{\partial \lambda}, \tag{4a}$$

$$g = -\frac{\partial \psi}{\partial \gamma}. \tag{4b}$$

The internal energy

$$e(\lambda, \gamma, \dot{\alpha}) = \psi + \dot{\alpha}s \tag{5}$$

is obtained by the Legendre transformation of the free energy $\psi$ with respect to the temperature $\dot{\alpha}$. Further relations that will be utilized later are

$$\dot{\mathbf{q}} = \frac{\partial \tilde{T}}{\partial \mathbf{p}}, \tag{6a}$$

$$\dot{\alpha} = \frac{\partial \tilde{e}}{\partial s}, \tag{6b}$$

where $\tilde{T}(\mathbf{q}, \mathbf{p})$ is the kinetic energy and $\tilde{e}(\lambda, \gamma, s)$ denotes the internal energy as a function of $(\lambda, \gamma, s)$.

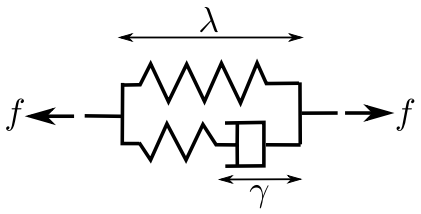


FIG. 1. Generalized Maxwell element

## III. TIME DISCRETIZATION

The problems adressed in this paper are nonlinear in nature, and usually only numerical solutions can be obtained. Three structure-preserving time integration schemes will be described in this section: a VI, an EEM method in entropy formulation (Gs) and in temperature formulation (GT). All of them aim at good longtime behavior and improved numerical stability in comparison to standard methods for ordinary differential equations.

### A. Variational Integrators

Variational integrators are based on a discrete version of Hamilton's principle of stationary action. To formulate them, the essential step is thus to write the action functional, from which the method follows naturally. For conservative mechanical problems, this choice is standard. However, the inclusion of dissipative effects (viscosity and Fourier's heat transfer) requires the use of incremental potentials [26] or the use of D'Alembert terms [25]. In this article we follow the latter option.

In this section the classical Hamilton principle is extended to encompass thermomechanics. Based on this principle, variational integrators are constructed in a systematic fashion. More specifically, the action is approximated with a discrete action evaluated as a quadrature based on the midpoint rule (MP). The resulting method, which we refer to as "variational mid-point", is not to be mistaken with the conventional time integration scheme. The generalization to higher order integrators will be discussed at the end of this section.

### 1. Variational Formulation

The classical Hamilton principle reads

$$\delta S = \delta \int_{t_0}^{t_1} L \,\mathrm{d}t = \delta \int_{t_0}^{t_1} (T - V) \,\mathrm{d}t = 0, \tag{7}$$

where $L, T, V$ are, respectively, the Lagrangian, the kinetic and the potential energies. The extension of this principle to thermoelasticity is obtained by replacing the potential energy $V(\mathbf{q})$ by the free energy $\psi(\lambda, \gamma, \vartheta)$ [18]. The use of thermacy as variable makes the resulting Euler-Lagrange equations of the thermal problem to take the same mathematical structure as the mechanical

$$\frac{\mathrm{d}}{\mathrm{d}t}\frac{\partial L}{\partial \dot{\mathbf{q}}} - \frac{\partial L}{\partial \mathbf{q}} = 0, \tag{8a}$$

$$\frac{\mathrm{d}}{\mathrm{d}t}\frac{\partial L}{\partial \dot{\alpha}} - \frac{\partial L}{\partial \alpha} = 0. \tag{8b}$$

These equations refer to the conservative case. In order to include nonconservative generalized forces, Hamiltons principle is enhanced by D'Alembert terms [25]

$$\delta \int_{t_0}^{t_1} L \,\mathrm{d}t + \int_{t_0}^{t_1} \delta W^{\mathrm{nc}} \,\mathrm{d}t = 0, \tag{9}$$

where $\delta W^{\mathrm{nc}}$ splits into mechanical and thermal contributions

$$\delta W^{\mathrm{nc}}_{\mathrm{mech}} = \mathbf{f} \cdot \delta \mathbf{q}, \qquad \delta W^{\mathrm{nc}}_{\mathrm{therm}} = \dot{s}\delta\alpha. \tag{10}$$

These terms account for mechanical forces such as external forcing or damping and for entropy fluxes, also called "thermal forces" that stem from heat production (external source) or from heat transfer by Fourier's law.

### 2. Construction of Variational Integrators

The construction of a variational integrator starts directly from the variational principle. It consists of two steps. Firstly, the functions of the generalized coordinates $\mathbf{q}(t)$ are discretized by interpolation functions $\mathbf{q}_d(t)$. Secondly, a quadrature rule for the evaluation of the action integral is applied. For the sake of simplicity the following explanations refer exemplarically to linear interpolation

$$\mathbf{q}(t) \approx \mathbf{q}_d(t) = \frac{t^{k+1} - t}{t^{k+1} - t^k}\mathbf{q}^k + \frac{t - t^k}{t^{k+1} - t^k}\mathbf{q}^{k+1}, \tag{11a}$$

$$\dot{\mathbf{q}}(t) \approx \dot{\mathbf{q}}_d(t) = \frac{\mathbf{q}^{k+1} - \mathbf{q}^k}{t^{k+1} - t^k} \quad \text{for} \quad t \in [t^k, t^{k+1}], \tag{11b}$$

and numerical integration by the midpoint rule

$$\int_{t^k}^{t^{k+1}} L\big(\mathbf{q}_d(t), \dot{\mathbf{q}}_d(t)\big) \,\mathrm{d}t \approx \underbrace{hL\big(\mathbf{q}_d(t^{k+1/2}), \dot{\mathbf{q}}_d(t^{k+1/2})\big)}_{L_d(\mathbf{q}^k, \mathbf{q}^{k+1})}, \tag{12}$$

where $h = t^{k+1} - t^k$ denotes the time step size, $t^{k+1/2} = t^k/2 + t^{k+1}/2$ half-time and $L_d$ is called discrete Lagrangian. As a result of this step, the continuous variational problem is turned into a discrete one, one requiring the stationarity of the discrete action sum

$$S_d = (\mathbf{q}^0, \ldots, \mathbf{q}^N) = \sum_{k=0}^{N-1} L_d(\mathbf{q}^k, \mathbf{q}^{k+1}) \tag{13}$$

plus discrete D'Alembert terms

$$\delta W^{nc} = \int_{t_1}^{t_2} \mathbf{f}_d \cdot \delta\mathbf{q} + \dot{s}\delta\alpha \,\mathrm{d}t \tag{14a}$$

$$\approx \sum_{k=0}^{N-1} h\big(\mathbf{f} \cdot \delta\mathbf{q} + \dot{s}\delta\alpha\big)|_{t=t_k+1/2} = \delta W_d^{nc} \tag{14b}$$

to vanish. The discrete forces, likewise the discrete Lagrangian, are obtained by numerical integration. If again the midpoint rule is applied to the time integral, now of the virtual work, then the force during one time step is split into discrete values, one at the beginning and the other at the end of the time step. Thus at each time point, except the first and the last one, two forces enter the equation, one originating from the previous time step and the other from the next time step

$$\mathbf{f}_d^+(\mathbf{q}^{k-1}, \mathbf{q}^k) = \int_{t^{k-1}}^{t^k} \mathbf{f}(t)\frac{\partial \mathbf{q}_d(t)}{\partial \mathbf{q}^k}\mathrm{d}t = \frac{h\mathbf{f}(t^{k-1/2})}{2}, \tag{15a}$$

$$\mathbf{f}_d^-(\mathbf{q}^k, \mathbf{q}^{k+1}) = \int_{t^k}^{t^{k+1}} \mathbf{f}(t)\frac{\partial \mathbf{q}_d(t)}{\partial \mathbf{q}^k}\mathrm{d}t = \frac{h\mathbf{f}(t^{k+1/2})}{2}, \tag{15b}$$

as deduced from the Discrete D'Alembert principle [25]. Evaluating the stationarity condition (14a)

$$0 = \sum_{k=0}^{N-1} \delta L_d(\mathbf{q}^k, \mathbf{q}^{k+1}) + \sum_{k=0}^{N-1} \delta W_d^{nc}(\mathbf{q}^k, \mathbf{q}^{k+1}) \tag{16}$$

results in the $N$ discrete Euler-Lagrange equations for all admissable positions $\mathbf{q}^1 \ldots \mathbf{q}^N$. The shorthand symbol $D_i$ will be used in the following to denote derivation with respect to the $i$th argument, i.e. $D_1 L_d(\mathbf{q}^k, \mathbf{q}^{k+1}) = \frac{\partial L_d}{\partial \mathbf{q}^k}$. The first equation

$$D_2 L(\mathbf{q}^0, \dot{\mathbf{q}}^0) = -D_1 L_d(\mathbf{q}^0, \mathbf{q}^1) - \mathbf{f}_d^-(\mathbf{q}^0, \mathbf{q}^1) \tag{17}$$

determines $\mathbf{q}^1$ from the initial position $\mathbf{q}(t^0) = \mathbf{q}^0$ and initial velocity $\dot{\mathbf{q}}(t^0) = \dot{\mathbf{q}}^0$. While for $k = 1 \ldots N-1$ the remaining positions $\mathbf{q}^{k+1}$ follow recursively from

$$\begin{aligned} 0 = \; & D_2 L_d(\mathbf{q}^{k-1}, \mathbf{q}^k) + \mathbf{f}_d^+(\mathbf{q}^{k-1}, \mathbf{q}^k) \\ & + D_1 L_d(\mathbf{q}^k, \mathbf{q}^{k+1}) + \mathbf{f}_d^-(\mathbf{q}^k, \mathbf{q}^{k+1}). \end{aligned} \tag{18}$$

Introducing the following definitions

$$\mathbf{p}^k = -D_1 L_d(\mathbf{q}^k, \mathbf{q}^{k+1}) - \mathbf{f}_d^-(\mathbf{q}^k, \mathbf{q}^{k+1}), \tag{19a}$$

$$\mathbf{p}^{k+1} = +D_2 L_d(\mathbf{q}^k, \mathbf{q}^{k+1}) + \mathbf{f}_d^+(\mathbf{q}^k, \mathbf{q}^{k+1}), \tag{19b}$$

results in the position-momentum form. This name is justified, because the $\mathbf{p}^k$ are the discrete analogues to momenta and fullfil a discrete version of Noether's theorem [14]. Equation (19a) is then solved iteratively with tangent matrix

$$\mathbf{T} = D_2 D_1 L_d(\mathbf{q}^k, \mathbf{q}^{k+1}) - D_2 \mathbf{f}_d^-(\mathbf{q}^k, \mathbf{q}^{k+1}) \tag{20}$$

by a Newton scheme. The resulting $\mathbf{q}^{k+1}$ are just inserted into eq. (19b) in order to update the momentum. Then the procedure repeats for the next time step.

Higher order of the approximation increases the number of unknowns. For quadratic polynomials

$$q_d(t) = at^2 + bt + q^0 \qquad \text{with} \tag{21a}$$

$$a = \frac{2q^0 + 2q^1 - 4q^{1/2}}{h^2}, \tag{21b}$$

$$b = \frac{4q^{1/2} - 3q^0 - q^1}{h}, \tag{21c}$$

the unknows are $q^{1/2}$ and $q^1$, since the value $q^0$ at the beginning of the time step is known. A matching numerical integration is given by Simpson's rule

$$L_d = \frac{h}{6}\left(L|_{t=t^k} + 4L|_{t=t^{k+1/2}} + L|_{t=t^{k+1}}\right). \tag{22}$$

Evaluation of the variation results in the same number of Euler-Lagrange equations as the number of unknowns, here for the conservative part

$$\begin{aligned} \mathbf{0} \;=\; & D_3 L_d(\mathbf{q}^{k-1}, \mathbf{q}^{k-1/2}, \mathbf{q}^k) \\ & + D_1 L_d(\mathbf{q}^k, \mathbf{q}^{k+1/2}, \mathbf{q}^{k+1}), \end{aligned} \tag{23a}$$

$$\mathbf{0} = D_2 L_d(\mathbf{q}^{k-1}, \mathbf{q}^{k-1/2}, \mathbf{q}^k). \tag{23b}$$

Including nonconservative forces and expressing in position-momentum form yields the resulting equation system

$$\mathbf{p}^k = -D_1 L_d(\mathbf{q}^k, \mathbf{q}^{k+1/2}, \mathbf{q}^{k+1}) - \mathbf{f}_d^k, \tag{24a}$$

$$\mathbf{0} = +D_2 L_d(\mathbf{q}^k, \mathbf{q}^{k+1/2}, \mathbf{q}^{k+1}) + \mathbf{f}_d^{k+1/2}, \tag{24b}$$

$$\mathbf{p}^{k+1} = +D_3 L_d(\mathbf{q}^k, \mathbf{q}^{k+1/2}, \mathbf{q}^{k+1}) + \mathbf{f}_d^{k+1}, \tag{24c}$$

consisting of a nonlinear part, eqns. (24a)-(24b), which must be solved iteratively and an update equation (24c). While the first and last equation give the stepping from one time step to the next, the second equation expresses the stationarity condition of the action during one time step. Combining quadratic approximations with a Lobatto quadrature formula of third-order leads to a forth-order accurate VI scheme whereas the combination of linear approximation and mid-point rule is second-order accurate.

The state variables $\mathbf{q}$, $\mathbf{p}$ are calculated directly by the variational integrator. In contrast to mechanical position, thermacy is merely used for the derivation of the time stepping scheme, its absolute values are typically of little interest and hence not stored in simulations. In order to obtain dependent quantitaties $\dot{\mathbf{q}}$, i.e. velocity and temperature, their definitions by eqs. (6a)-(6b) are rather evaluated than the time derivatives of their approximations. These values are better in terms of structure preservation than the interpolations, whose time-derivatives are not necessarily continous at the time nodes. Similarly the kinetic energy $T$ and internal energy $e$ are evaluated as functions of the state variables $\mathbf{q}$, $\mathbf{p}$. If these relations cannot be evaluated analytically, e.g. the Legendre transform does not provide an analytical expression for the velocities as function of the momenta, they still can be evaluated numerically.

One of the most important aspects of variational integrators is backward error analysis. It predicts the characteristics of the discrete-time path rather than the rate of convergence. Considering the discretization of a Hamiltonian system by a variational integrator results in discrete states that are the exact solutions to a nearby Hamiltonian system [9]

$$\tilde{H}(\mathbf{q}, \mathbf{p}) = H(\mathbf{q}, \mathbf{p}) + \frac{h^2}{2!} g_1(\mathbf{q}, \mathbf{p}) + \frac{h^4}{4!} g_2(\mathbf{q}, \mathbf{p}) + \ldots, \tag{25}$$

where $H$ denotes the original Hamiltonian. The functions $g_i$ can be determined using the method of modified equations [8]. Even though the conservation of the original Hamiltonian is incompatible with symplecticity, the energy error remains bounded [9]. Variational integrators are symplectic as long as the time steps are equidistant.

Note that besides conservative forces variational integrators can handle both external forcing and dissipation [14] and proved well suited for practical applications in robotics [11] and also to be demonstrated by the following examples in this paper.

### B. Energy-Entropy-Momentum Methods

For general, finite-dimensional isolated thermodynamic systems, the time-evolution of the state variables arranged in $\mathbf{z}$, may be expressed by the following initial-value problem

$$\dot{\mathbf{z}} = \mathbf{L}(\mathbf{z})\nabla E(\mathbf{z}) + \mathbf{M}(\mathbf{z})\nabla S(\mathbf{z}), \quad \mathbf{z}(0) = \mathbf{z}_0 \tag{26}$$

$E$ being the total energy and $S$ being the total entropy, $\nabla(\bullet)$ being the gradient operator with respect to the state space vector, $\mathbf{z}_0$ containing the prescribed initial conditions and $\mathbf{L}, \mathbf{M}$ being the so-called Poisson matrix and the Dissipative matrix, respectively. The evolution equations (26) will be in accordance with the laws of thermodynamics provided that the Poisson and Dissipative matrices are skew-symmetric and symmetric, positive semi-definite, respectively, and satisfy the degeneracy conditions

$$\nabla S^{\mathrm{T}} \mathbf{L} = \mathbf{0}, \quad \nabla E^{\mathrm{T}} \mathbf{M} = \mathbf{0}. \tag{27}$$

The proof is straightforward and can be found in [16].

Following the guidelines in Romero [21], the discrete derivative operator, denoted as $\mathsf{D}(\bullet)(\mathbf{z}^{k+1},\mathbf{z}^k)$, is employed to arrive at the following monolithic implicit second order accurate method

$$\begin{aligned}\frac{\mathbf{z}^{k+1}-\mathbf{z}^k}{h} &= \mathbf{L}(\mathbf{z}^{k+1},\mathbf{z}^k)\mathsf{D}E(\mathbf{z}^{k+1},\mathbf{z}^k)\\ &+ \mathbf{M}(\mathbf{z}^{k+1},\mathbf{z}^k)\mathsf{D}S(\mathbf{z}^{k+1},\mathbf{z}^k)\end{aligned} \tag{28}$$

where the $\mathbf{L}(\mathbf{z}^{k+1},\mathbf{z}^k)$, $\mathbf{M}(\mathbf{z}^{k+1},\mathbf{z}^k)$ are second order approximations of the above Poisson and Dissipative matrices and, therefore, have their respective properties. Particularly, the degeneracy conditions are fulfilled in the following way

$$\mathbf{0} = \mathsf{D}S(\mathbf{z}^{k+1},\mathbf{z}^k)^{\mathrm{T}}\mathbf{L}(\mathbf{z}^{k+1},\mathbf{z}^k), \tag{29a}$$

$$\mathbf{0} = \mathsf{D}E(\mathbf{z}^{k+1},\mathbf{z}^k)^{\mathrm{T}}\mathbf{M}(\mathbf{z}^{k+1},\mathbf{z}^k). \tag{29b}$$

The *discrete* laws of thermodynamics are thus satisfied due to these properties and the directionality property of the discrete derivative operator that allows to express the balance of any function in any time-step as

$$E^{k+1}-E^k = \mathsf{D}E\left(\mathbf{z}^{k+1},\mathbf{z}^k\right)\cdot(\mathbf{z}^{k+1}-\mathbf{z}^k) \tag{30}$$

that can be further elaborated using (28) to give

$$\begin{aligned}&E^{k+1}-E^k\\ &= h\mathsf{D}E(\mathbf{z}^{k+1},\mathbf{z}^k)^{\mathrm{T}}\mathbf{L}(\mathbf{z}^{k+1},\mathbf{z}^k)\mathsf{D}E(\mathbf{z}^{k+1},\mathbf{z}^k)\\ &+ h\mathsf{D}E(\mathbf{z}^{k+1},\mathbf{z}^k)^{\mathrm{T}}\mathbf{M}(\mathbf{z}^{k+1},\mathbf{z}^k)\mathsf{D}S(\mathbf{z}^{k+1},\mathbf{z}^k) = 0.\end{aligned} \tag{31}$$

Similarly, the total entropy balance results in

$$\begin{aligned}&S^{k+1}-S^k\\ &= \mathsf{D}S\left(\mathbf{z}^{k+1},\mathbf{z}^k\right)\cdot(\mathbf{z}^{k+1}-\mathbf{z}^k)\\ &= h\mathsf{D}S(\mathbf{z}^{k+1},\mathbf{z}^k)^{\mathrm{T}}\mathbf{L}(\mathbf{z}^{k+1},\mathbf{z}^k)\mathsf{D}E(\mathbf{z}^{k+1},\mathbf{z}^k)\\ &+ h\mathsf{D}S(\mathbf{z}^{k+1},\mathbf{z}^k)^{\mathrm{T}}\mathbf{M}(\mathbf{z}^{k+1},\mathbf{z}^k)\mathsf{D}S(\mathbf{z}^{k+1},\mathbf{z}^k)\geq 0.\end{aligned} \tag{32}$$

The method (28) also ensures the conservation of quadratic momentum maps if the discrete derivative is modified to account for the symmetries in the system. Details and proofs of this statement can be found in [21].

When specifying the presented approach, the Poisson and Dissipative matrices need to be fully defined. In doing so, a crucial issue in the formulation raises regarding the choice for the thermodynamic variables. Thus, in the very beginning of EEM methods the use of entropy variables was favored, as it easily provides the matrices and, therefore, thermodynamically consistent methods were straightforwardly achieved, although assuming significant restrictions in the formulation, such as difficulties for temperature boundary conditions. The recent work [19] concluded that a temperature-based formulation can also provide the GENERIC matrices, facilitating the formulation of thermodynamically consistent methods based on temperature variables, see [16], and thus overcoming the mentioned restrictions. In the following subsections we summarize the main aspects of both formulations for the model presented in Section II.

### 1. *Energy-Entropy-Momentum Methods in Entropy Formulation*

As previously pointed out, the GENERIC formulation only applies to isolated systems, i.e. the element and the environment with which it exchanges heat must be considered as the thermodynamic system. To this end, the easiest way is to consider the environment to have a constant temperature $\vartheta_\infty$. Thus the system is thermomechanically determined by means of five independent variables, among which both the element and the environment entropies $s$ and $s_\infty$ must be included to achieve an entropy-based formulation, that is

$$\mathbf{z} = [\mathbf{q},\mathbf{p},\gamma,s,s_\infty] \tag{33}$$

This choice simplifies the Poisson matrix to be the classical symplectic one, see [1], and the Dissipative matrix gets not too involved, enabling such a straightforward formulation that it was achieved in [6] with no need for the GENERIC form to reveal the structure meant to be preserved.

However, this formulation is valid provided that the relations $\vartheta = \vartheta(\lambda,\gamma,s)$ could be analytically found. For standard temperature-based free energy functions [5], this consideration limits the thermo-elastic parameters of the model to be at most linearly temperature-dependent.

### 2. *Energy-Entropy-Momentum Methods in Temperature Formulation*

To avoid this issue, a temperature-based formulation becomes crucial, for which the element and the environment temperatures should be considered as state variables

$$\mathbf{z} = [\mathbf{q},\mathbf{p},\gamma,\vartheta,\vartheta_\infty] \tag{34}$$

Note that this choice implies the environment temperature $\vartheta_\infty$ to be non-constant so that the environment internal energy in terms of it, $\epsilon(\vartheta_\infty)\colon \mathbb{R}^+ \to \mathbb{R}$, can be defined. With this consideration, the GENERIC matrices become more intricate but affordable (see [15]), thus allowing to formulate a temperature-based thermodynamically consistent counterpart which overcomes the restrictions related to the entropy formulation pointed out before.

## IV. NUMERICAL EXAMPLES

The two classes of integrators introduced in the previous section, variational integrators and EEM methods, are now to be applied to model problems from the literature: a planar thermo-viscoelastic single pendulum [6] and a spatial thermo-elastic double pendulum [16]. The former compares a second-order accurate VI with a

second-order accurate EEM method in entropy formulation whereas the latter compares the same VI with an EEM method in temperature formulation.

### A. Planar Thermo-Viscoelastic Single Pendulum with Classical Heat Conduction with the Environment

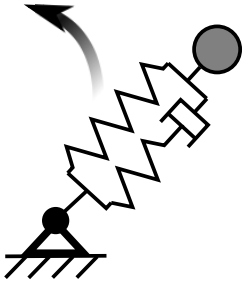

FIG. 2. example 1: a mass attached to a massless thermo-viscoelastic spring with heat transfer with the environment

This planar pendulum shown in Fig. 2 is taken from the literature [6]. The length of the massless pendulum rod

$$\lambda = \sqrt{x^2 + y^2} \tag{35}$$

depends on the position $(x, y)$ of the attached mass. The evolution equation of the dash-pot is assumed to be linear

$$\eta\dot{\gamma} = g, \tag{36}$$

where $\gamma$ denotes stretch of the dash-pot and $g$ the corresponding viscous force (4b). The free energy, defined generally by eq. (2), is specified by thermo-elastic springs with

$$\begin{aligned}\psi_e(\lambda, \dot{\alpha}) = \; & \frac{k}{2}\log^2\left(\tfrac{\lambda}{\lambda_0}\right) - \beta_t(\dot{\alpha} - \vartheta_r)\log\left(\tfrac{\lambda}{\lambda_0}\right) \\ & + c\left[\dot{\alpha} - \vartheta_r - \dot{\alpha}\log\left(\tfrac{\dot{\alpha}}{\vartheta_r}\right)\right],\end{aligned} \tag{37}$$

where $k$ denotes the elasticity coefficient, which is related with stiffness, of the main spring, $\beta_t$ the thermomechanical coupling parameter, which is related with thermal expansion, and $c$ the heat capacity. This free energy function allows for large strains and Gough-Joule coupling. Its parameters are summarized in tab. I for convenience.

The thermal part is the heat transfer between spring and environment and the heat generated by the dash-pot. The heat transfer is modeled by Fourier's law

$$\phi = -\kappa(\dot{\alpha} - \vartheta_\infty), \tag{38}$$

where the environment is assumed to be a thermal reservoir of constant temperature $\vartheta_\infty$. Regarding the dash-pot, it is assumed that all energy mechanically dissipated is completely converted into heat, which corresponds to the entropy production

$$\dot{s}_v = \frac{g\dot{\gamma}}{\dot{\alpha}}. \tag{39}$$

The expression for the virtual work of the nonconservative forces thus consists of three summands

$$\delta W^{nc} = -g\delta\gamma + \frac{g\dot{\gamma}}{\dot{\alpha}}\delta\alpha + \kappa\frac{\dot{\alpha} - \vartheta_\infty}{\dot{\alpha}}\delta\alpha \tag{40}$$

done by the viscous force of the dash-pot, heat generated by the dash-pot and heat conduction with the environment. Both, energy and entropy of the environment are assumed zero initially.

The free motion for given initial conditions is taken as example. The linearization around the unstretched position at rest and at reference temperature indicates free oscillations of period $t_{\text{period}} = 0.086$s and gives an idea ot the motions time scale.

Using the same time step $h = 0.2$s as in the reference [6] results, after 3-4 Newton-iterations per time step, in trajectories and time histories of position and temperature that are indistinguishable.

Thus the focus is now on the conservation properties. Fig. 3 shows how the numerically obtained total energy deviates from the exact value that is known to be constant on physical grounds. As expected the EEM scheme outperforms the variational integrator in terms of energy as listed in tab. III. The entropy is, as usual for diffusion processes in which temperatures level out, a monotonically increasing function asymptotically approaching its upper bound. Fig. 4 shows the deviations of the total entropy compared to a reference trajectory much finer discretized than the other results ($h = 0.005$s), both integrators show oscillatory deviations settling to the final value. The entropy rates are not shown additionally, as they are in accordance with the second law, i.e. strictly increasing for all the simulations, which is an inherent characteristic of both schemes.

Both integrators calculate the angular momentum, which is to be constant in this model, within machine precision.

Comparisons with standard solvers are not feasible since they get instable at this step size as documented in [6].

### B. Spatial Thermo-elastic Double Pendulum with Classical Heat Conduction

This example, shown in fig. 5, is taken from Conde [16]. Its free energy is again given by eq. (37), but its parameters, listed in tab. II are not only different in value but also in their functional dependencies. Particularly the logarithmic term in the elasticity coefficient turns the relation between entropy $s$ and temperature $\dot{\alpha}$ into a transcendental equation. This makes the decisive difference

TABLE I. Single pendulum parameters (example 1)

| | | | |
|---|---|---|---|
| $m$ | 1 | kg | mass |
| $\lambda_0$ | 1 | m | unstretched length |
| $k(\vartheta)$ | $k_0 - k_1(\vartheta - \vartheta_r)$ | | elasticity coefficient |
| $k_0$ | 100 | Nm | |
| $k_1$ | 0.5 | Nm/K | |
| $\beta_c$ | 0.1 | | spring ratio |
| $\beta_t$ | 4 | Nm/K | thermoelastic coupling |
| $c$ | 1 | Nm/K | heat capacity |
| $\mu(\vartheta)$ | $\mu_0 - \mu_1(\vartheta - \vartheta_r)$ | | viscosity coefficient |
| $\mu_0$ | 5 | N/m | |
| $\mu_1$ | 0.1 | N/mK | |
| $\eta(\vartheta)$ | $\eta_0 e^{a(1/\vartheta - 1/\vartheta_r)}$ | | viscosity |
| $\eta_0$ | 100 | Ns/m | |
| $a$ | 10 | K | |
| $\kappa$ | 10 | W/K | thermal conductivity |
| $\vartheta_r$ | 300 | K | reference temperature |
| $\vartheta_\infty$ | 300 | K | environment temperature |
| $\mathbf{q}_0$ | $[3, 0]$ | m | initial position |
| $\dot{\mathbf{q}}_0$ | $[0, 1]$ | m/s | initial velocity |
| $\gamma_0$ | 0 | m | initial viscous stretch |
| $\vartheta_0$ | 380 | K | initial temperature |
| $t_{\text{sim}}$ | 20 | s | simulation time |
| $h$ | 0.2 | s | time step |
| $\varepsilon$ | $10^{-10}$ | | Newton tolerance for Euclidean norm $\lvert\Delta\mathbf{z}\rvert$ |

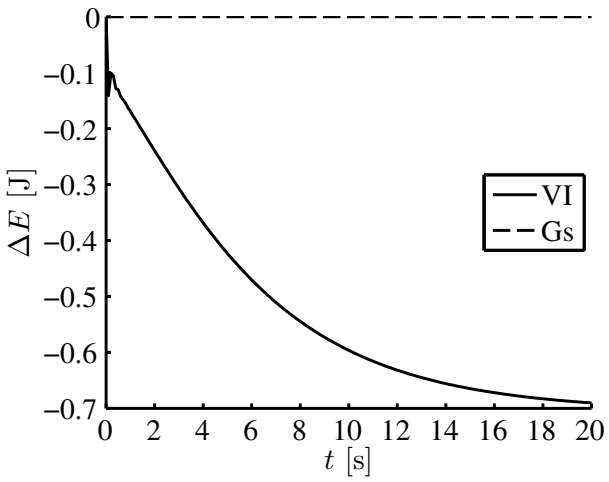


FIG. 3. example 1: error in total energy ($E$ = const. = $1704J$) vs. time for the variational integrator (VI) and the EEM method (Gs)

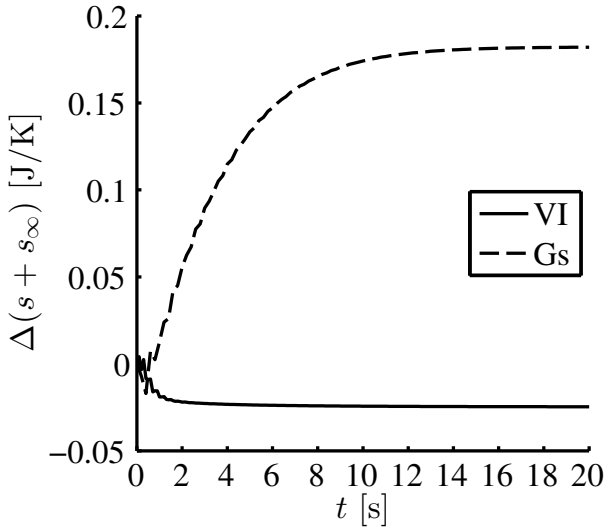


FIG. 4. example 1: error in total entropy ($s + s_\infty$ = $5.4258 \ldots 5.4613$J/K) vs. time for the variational integrator (VI) and the Energy-Entropy-Momentum method (Gs)

compared to the previous example, the Legendre transform gets more involved, since there is no more analytical expression for temperature as function of entropy. As a consequence, the EEM method in entropy formulation is ruled out.

The thermal system contains heat transfer between the springs but not with the environment. The heat fluxes from spring 1 into spring 2 and vice versa are again modeled by Fourier's law

$$\phi_1 = -\kappa(\vartheta_1 - \vartheta_2) = -\kappa(\dot{\alpha}_1 - \dot{\alpha}_2), \tag{41a}$$
$$\phi_2 = -\phi_1. \tag{41b}$$

Thus, the double pendulum forms an isolated system and its total energy $E = T + e$ is to be conserved.

The system linearized around the state of rest in vertical hanging position and at average temperature indicates a minimum period of free oscillations $t_{\text{period}} = 0.17$s, which gives an orientation for setting the time step.

Using the same time step $h = 0.1$s as Conde [16] makes the trajectories coincide in the beginning but diverge at about half-time ($t = 12.5$s). This divergence is probably rather due to the chaotic behavior of the mechanical system than to the integrator. The temperatures shown in fig. 6 coincide well until the diverging mechanical behavior affects the temperatures by the relatively strong thermal coupling in this example. Thus, the focus is more set on energetic quantities. Fig. 7 shows total energy, which should be constant on physical grounds. As expected the EEM scheme outperforms the variational integrator.

The entropy in the discrete solution increases, as it should, in an isolated system. A reference solution is taken to be a trajectory obtained with a very small time step size ($h = 0.005$s). Fig. 8 shows that the variational integrator is closer to this reference trajectory than the EEM method. Both integrators are in accordance with the second law of thermodynamics by design.

As the VI inherently preserves momentum maps it is

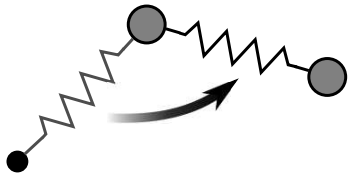

FIG. 5. example 2: thermo-elastic double pendulum with heat transfer between the springs

TABLE II. Double pendulum parameters (example 2)

| | | | |
|---|---|---|---|
| $m_1$ | 10 | kg | mass |
| $m_2$ | 20 | kg | mass |
| $\lambda_{0,1}$ | 2 | m | unstretched length |
| $\lambda_{0,2}$ | 1 | m | unstretched length |
| $k_i(\vartheta)$ | $k_{i0} - k_{i1}\vartheta_r \log(\vartheta_i/\vartheta_r)$ | | elasticity coefficient |
| $k_{10}$ | 5000 | J | |
| $k_{11}$ | 50 | J/K | |
| $k_{20}$ | 10000 | J | |
| $k_{21}$ | 60 | J/K | |
| $\beta_{t1}$ | 20 | J/K | thermoelastic coupling |
| $\beta_{t2}$ | 20 | J/K | thermoelastic coupling |
| $c_1$ | 5000 | J/K | heat capacity |
| $c_2$ | 2000 | J/K | heat capacity |
| $\kappa$ | 300 | W/K | thermal conductivity |
| $\vartheta_r$ | 300 | K | reference temperature |
| | | | |
| $\mathbf{q}_1(0)$ | $[3, 0, 0.5]^T$ | m | initial position |
| $\mathbf{q}_2(0)$ | $[3, 1, 1]^T$ | m | initial position |
| $\mathbf{p}_1(0)$ | $[0, 10, 0]^T$ | kg m/s | initial momentum |
| $\mathbf{p}_2(0)$ | $[0, 0, -20]^T$ | kg m/s | initial momentum |
| $\vartheta_1(0)$ | 380 | K | initial temperature |
| $\vartheta_2(0)$ | 298 | K | initial temperature |
| | | | |
| $t_{\text{sim}}$ | 25 | s | simulation time |
| $h$ | 0.1 | s | time step |
| $\varepsilon$ | $10^{-10}$ | | Newton tolerance for Euclidean norm $\lvert\Delta\mathbf{z}\rvert$ |

supposed to perform better in the balance of momentum. For the double pendulum the angular momentum is to be preserved and indeed in fig. 9 only the error of the EEM scheme is visible while the variational integrator stays within machine precision. In average, the variational integrator required one Newton iteration (3-4 iterations) less then the EEM-integrator (4-5 iterations). We note that a standard solver (mid-point rule with fixed step size) would have needed a time step size of less than $h = 0.01$s in order to stably integrate the motion. The relative errors for the simulations of both examples, double pendulum and single pendulum simulations, are listed in tab. III.

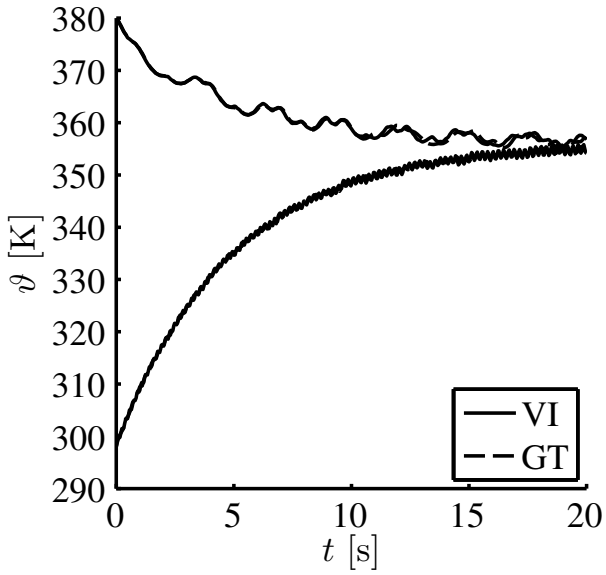


FIG. 6. Example 2: temperature vs. time for the variational integrator (VI) and the Energy-Entropy-Momentum method (GT)

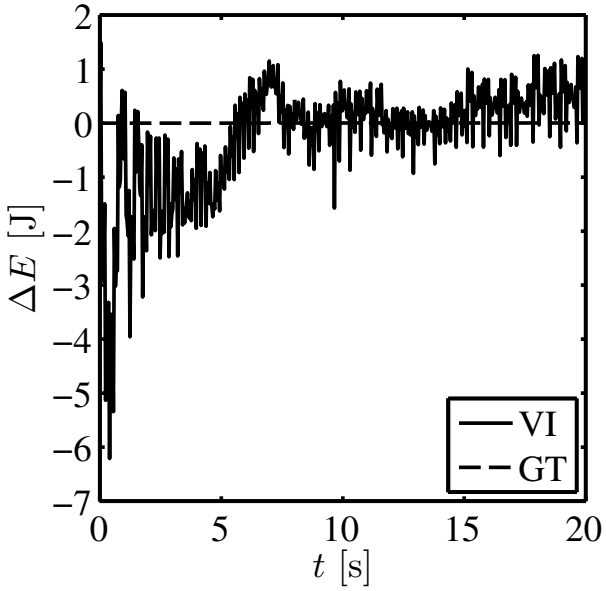


FIG. 7. Example 2: energy error ($E$ = const. = $4 \cdot 10^5$J) vs. time for the variational integrator (VI) and the Energy-Entropy-Momentum method (GT)

## V. SUMMARY AND OUTLOOK

Variational integrators (VI) have been extensively employed for approximating the evolution of Hamiltonian systems, leading to time integration schemes with remarkable, well-known, features. Similarly to Energy-Entropy-Momentum (EEM) methods, they demonstrate that structure preservation leads to time stepping

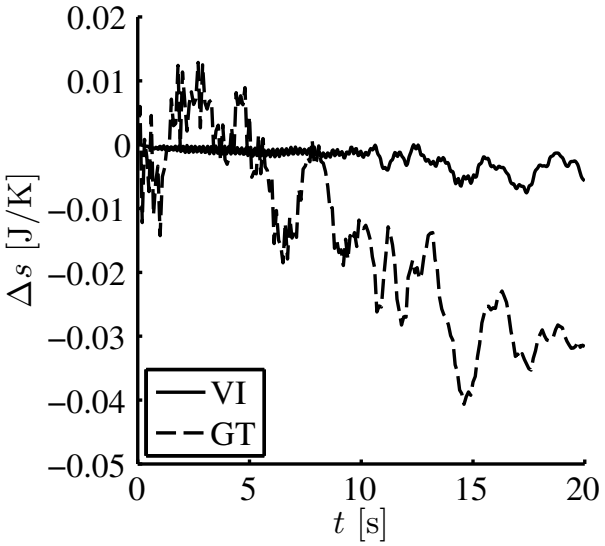


FIG. 8. Example 2: entropy ($s = 1183 \dots 1222$J/K) error vs. time for the variational integrator (VI) and the Energy-Entropy-Momentum method (GT)

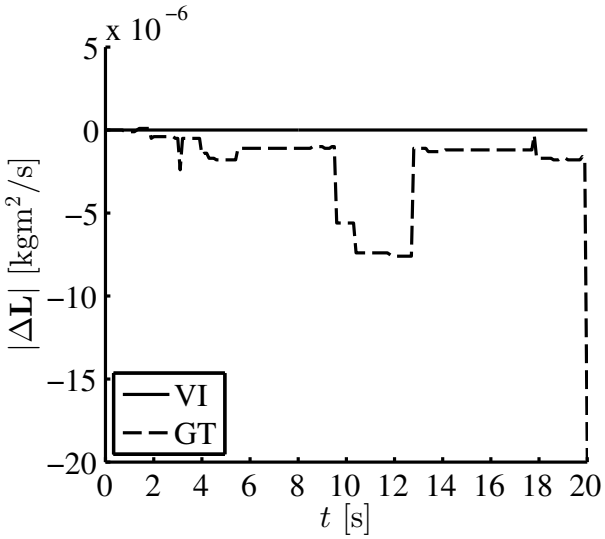


FIG. 9. Example 2: angular momentum ($|\mathbf{L}| = \text{const.} = 71.6\text{kgm}^2/\text{s}$) vs. time for the variational integrator (VI) and the Energy-Entropy-Momentum method (GT)

schemes that are more robust than standard ones, especially in stiff problems. Both time discretizations, VI and EEM methods, can employ time step sizes which are too large for standard solvers, and their long term behavior is much more accurate. In comparison to EEM methods, particularly in entropy formulation, the implementation of VIs poses no restrictions on boundary conditions and parameter dependencies for the time stepping itself. However, the postprocessing still may require further numerical evaluations.

Thermo-viscoelasticity is not covered by classical Hamiltonian mechanics. However, we have shown that viscous forces and heat transfer can be incorporated to the Hamiltonian action using D'Alembert terms. Comparison of the results for the discrete examples produced by same time steps shows the advantage of VI over EEM in momentum preservation, including entropy balance, on the one hand and the disadvantage of worse energy conservation on the other hand. This is not suprising, since EEMs are by design energy consistent and VIs known to preserve momentum maps exactly. In addition it is observed for VI methods that they not get worse when applied to dissipative systems, i.e. when extended by the Discrete D'Alembert principle, where symplecticity is lost.

TABLE III. Relative errors in examples 1 and 2 computed as ratio between maximal deviation from the reference trajectory divided by the mean value of the reference trajectory

| | energy | entropy | momentum |
|---|---|---|---|
| example 1: VI | $4 \cdot 10^{-4}$ % | $5 \cdot 10^{-4}$% | $1 \cdot 10^{-14}$% |
| example 1: Gs | $3 \cdot 10^{-15}$% | $3 \cdot 10^{-3}$% | $1 \cdot 10^{-15}$% |
| example 2: VI | $1 \cdot 10^{-3}$ % | $6 \cdot 10^{-4}$% | $7 \cdot 10^{-11}$% |
| example 2: GT | $1 \cdot 10^{-12}$% | $3 \cdot 10^{-3}$% | $3 \cdot 10^{-5}$ % |

A general comment on both VI and EEM methods is that both, GENERIC-based and variational, demonstrate that structure preservation leads to algorithms more robust than standard ones. As disadvantage they share the strong interlocking between physics and numerics making the implementation problem specific.

Further works aims at algorithmic speedup and simplification by separating and modularizing these integrators as much as possible. Yet another possible line of improvement is the development of splitting methods that separate the governing equations of the problem into implicit and explicit blocks. Incremental potentials [26] may be useful for this goal as well as methods based on the discrete Pontryagin principle [13].

[1] Alan J L, Meyer K (1972) Canonical forms for symplectic and Hamiltonian matrices. Celestial Mechanics 9(1974):213–238
[2] Bertram A (2013) Festkörpermechanik. Otto-von-Guericke-Universität Magdeburg
[3] Cadzow JA (1970) Discrete calculus of variations. International Journal of Control 11(3):393–407
[4] Crandall SH (1968) Dynamics of mechanical and electromechanical systems. McGraw-Hill
[5] Dillon O (1962) A nonlinear thermoelasticity theory. Journal of the Mechanics and Physics of Solids 10(2):123–131

[6] García Orden JC, Romero I (2012) Energy-entropy-momentum integration of discrete thermo-visco-elastic dynamics. European Journal of Mechanics-A/Solids 32:76–87

[7] Gonzalez O (1996) Time integration and discrete hamiltonian systems. Journal of Nonlinear Science 6(5):449–467

[8] Griffiths D, Sanz-Serna J (1986) On the scope of the method of modified equations. SIAM Journal on Scientific and Statistical Computing 7(3):994–1008

[9] Hairer E, Lubich C, Wanner G (2006) Geometric numerical integration: structure-preserving algorithms for ordinary differential equations, vol 31. Springer Science & Business Media

[10] Holzapfel GA, Simo JC (1996) A new viscoelastic constitutive model for continuous media at finite thermomechanical changes. International Journal of Solids and Structures 33(20):3019–3034

[11] Johnson ER, Murphey TD (2009) Scalable variational integrators for constrained mechanical systems in generalized coordinates. Robotics, IEEE Transactions on 25(6):1249–1261

[12] Kern D, Bär S, Groß M (2014) Variational integrators for thermomechanical coupled dynamic systems with heat conduction. Proceedings in Applied Mathematics and Mechanics

[13] Kharevych L, Yang W, Tong Y, Kanso E, Marsden JE, Schröder P, Desbrun M (2006) Geometric, variational integrators for computer animation. In: Proceedings of the 2006 ACM SIGGRAPH/Eurographics symposium on Computer animation, Eurographics Association, pp 43–51

[14] Marsden JE, West M (2001) Discrete mechanics and variational integrators. Acta Numerica 2001 10:357–514

[15] Martin SC, Garcia-Orden JC (2015) On generic-based integration methods for discrete thermo-visco-elastodynamics. Submitted to C&S –:–

[16] Martin SC, Betsch P, Garcia-Orden JC (2015) A temperature-based thermodynamically consistent integration scheme for discrete thermo-elastodynamics. Communications in Nonlinear Science and Numerical Simulation 32:63–80

[17] Mata P, Lew AJ (2011) Variational time integrators for finite-dimensional thermo-elasto-dynamics without heat conduction. International Journal for Numerical Methods in Engineering 88(1):1–30

[18] Maugin G, Kalpakides V (2002) A hamiltonian formulation for elasticity and thermoelasticity. Journal of Physics A: Mathematical and General 35(50):10,775

[19] Mielke A (2011) Formulation of thermoelastic dissipative material behavior using generic. Continuum Mechanics and Thermodynamics 23(3):233–256

[20] Öttinger HC (2005) Beyond equilibrium thermodynamics. John Wiley & Sons

[21] Romero I (2009) Thermodynamically consistent time-stepping algorithms for non-linear thermomechanical systems. International journal for numerical methods in engineering 79(6):706–732

[22] Romero I (2010) Algorithms for coupled problems that preserve symmetries and the laws of thermodynamics: Part i: Monolithic integrators and their application to finite strain thermoelasticity. Computer Methods in Applied Mechanics and Engineering 199(25):1841–1858

[23] Romero I (2010) Algorithms for coupled problems that preserve symmetries and the laws of thermodynamics: Part ii: Fractional step methods. Computer Methods in Applied Mechanics and Engineering 199(33):2235–2248

[24] Simo J, Tarnow N (1992) The discrete energy-momentum method. conserving algorithms for nonlinear elastodynamics. Zeitschrift für angewandte Mathematik und Physik ZAMP 43(5):757–792

[25] West M, Kane C, Marsden J, Ortiz M (2000) Variational integrators, the newmark scheme, and dissipative systems. Technical Report CalTech

[26] Yang Q, Stainier L, Ortiz M (2006) A variational formulation of the coupled thermo-mechanical boundary-value problem for general dissipative solids. Journal of the Mechanics and Physics of Solids 54(2):401–424